Climate-induced formation of a closed basin: Great Divide Basin, Wyoming

Paul L. Heller[1,†], Margaret E. McMillan[2], and Neil Humphrey[1]
[1]*Department of Geology and Geophysics, University of Wyoming, Laramie, Wyoming 82071, USA*
[2]*Department of Earth Sciences, University of Arkansas at Little Rock, Little Rock, Arkansas 72204, USA*

ABSTRACT

Large closed basins are often associated with regions of active tectonics. In contrast, we provide the example of the Great Divide Basin, in southern Wyoming, where climate change, through its impact on erosion and flexure, provides the primary mechanism of basin closure. Two- and three-dimensional flexural models that incorporate the effects of local basin abandonment due to aridity as well as minor extrabasinal extension demonstrate that basin closure with 40 m of basement relief (tilt) could have been achieved in the Great Divide Basin under reasonable assumptions of sediment rock density and flexural rigidity. The primary drive for basin abandonment was insufficient discharge that retarded river downcutting. Continued erosion in the surrounding drainage led to flexural rebound, against which erosion by the outlet from the Great Divide Basin was unable to compete. Eventually, the basin became detached and isolated from the surrounding drainage, and a few tens of meters of differential tilt developed between the basin floor and spillover point. An extra amount of tilt, up to a few meters, could have been attained by rift shoulder effects associated with minor nearby extension outside of the basin to the north. Hence, closure of the Great Divide Basin took place with no internal faulting, nor did it require any extrabasinal tectonic activity to force basin closure. Hence, basin closure and/or drainage reorganization need not record tectonic activity in all cases. Differential erosion provides an alternative hypothesis that does not reflect local tectonic timing. Our model of the evolution of the Great Divide Basin illustrates a mechanism by which basins can become closed by climatic effects alone.

INTRODUCTION

Large closed basins are typically associated with active tectonism in a variety of settings. Examples include Pyramid Lake, Nevada (with 109 m relief between basin floor and spillover point), in an extensional setting; Death Valley, California (148 m), in a strike-slip setting; and Qinghai Lake, north-central China (28 m), in a compressional setting. Such basins may be dry or contain lakes, depending on water supply (Carroll and Bohacs, 1999). In all cases, closed basin formation occurs where rates of sediment supply derived from surrounding mountain ranges lag behind rates of space created (accommodation) by tectonic activity in the basin (Carroll and Bohacs, 1999; Humphrey and Konrad, 2000; Garcia-Castellanos, 2007). Accommodation may result from basin subsidence or rate of surface uplift of a bounding tectonic sill. Typically, closed basins are geologically short-lived—once tectonism abates, continued sediment supply, coupled with erosional downcutting of the spillover point, eventually eliminates topographic barriers to drainage.

The Great Divide Basin of south-central Wyoming (Fig. 1) stands in contrast to closed basins formed in tectonically active settings. The basin is a large (~10^4 km^2), internally drained, topographic depression that sits at high elevation (2100 m average) astride the U.S. continental divide. With tens of meters of closure between basin floor and spillover point, the basin is as large as or larger than most closed basins. In this part of the Rocky Mountains, there is thought to be little recent tectonic activity (Flanagan and Montagne, 1993) and no known recent faulting within the basin. As such, an obvious tectonic origin of the Great Divide Basin is a difficult case to make. Alternatively, we suggest here that basin closure was primarily the result of an isostatic response to the climatically induced isolation of the basin from the surrounding drainages. Such a mechanism may play a role in other closed basins not directly controlled by active tectonism along their margins.

GREAT DIVIDE BASIN

The Great Divide Basin was originally part of a foreland basin bounded by the Sevier fold-and-thrust belt to the west during Cretaceous–early Eocene time. In Late Cretaceous time, the Laramide orogeny partitioned the foreland region into individual basins bounded by narrow basement-cored ranges (Snoke, 1993). This event produced the thrust-bounded ranges and domal uplifts that surround the Great Divide Basin today (Fig. 1). During the early part of the Laramide orogeny, the basin was a part of the greater Green River Basin (Surdam and Stanley, 1980). Subsequent relative uplift of the Rock Springs Uplift to the west and the Rawlins Uplift to the east (Fig. 1) during Late Cretaceous through Paleocene time further defined the margins of the Great Divide Basin (Lillegraven et al., 2002; Mederos et al., 2005). The basin was not closed, however, until at least middle to late Miocene time (Hansen, 1986; Lillegraven and Ostresh, 1988). Prior to this time, the basin drained to the east, into the Platte River system.

Continued, subtle, post-Laramide tectonism has affected the Rocky Mountains, including regional doming that began after 8 Ma and was well on its way by ca. 4 Ma (McMillan et al., 2006). Local post-Laramide tectonism and volcanism close to the Great Divide Basin include the extensional collapse of the Granite Mountains (beginning ca. 11–7 Ma; Anders et al., 2009) to the north, the propagation of the Rio Grande Rift to the east of the Sierra Madre Mountains (beginning 10–8 Ma; Mears, 1998; Keller and Baldridge, 1999), and eruption of the Leucite Hills (3–0.8 Ma; Lange et al., 2000) around the Rock Springs Uplift on the western margin of the basin.

It is unclear exactly when the Great Divide Basin became isolated from the Platte River drainage. Regional studies indicate that the basin and adjacent parts of the Northern Platte River drainage were buried under >600 m of Oligocene–Miocene basin fill after the end of

[†]E-mail: heller@uwyo.edu

GSA Bulletin; doi: 10.1130/B30113.1; 6 figures; 1 table; Data Repository item 2010158.

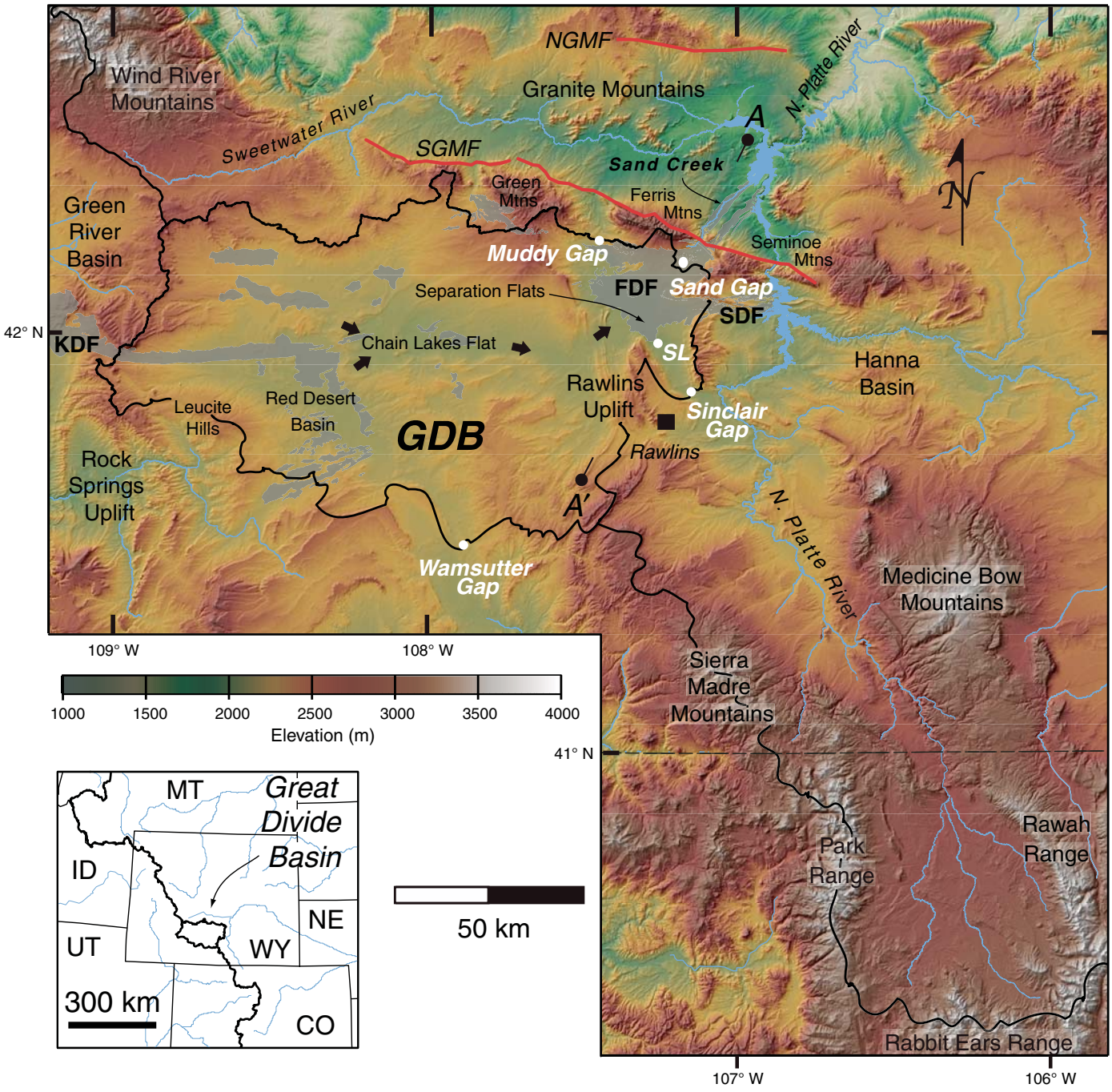

Figure 1. Location and topography of the Great Divide Basin (GDB), southern Wyoming. The basin is surrounded by the continental divide (bold line on inset map). Locations of likely outflows for the basin are shown in white. Young faults are shown in red (South Granite Mountain fault—SGMF; North Granite Mountain fault—NGMF). Gray shading shows location of significant sand dune deposits (KDF—Killpecker dune field; FDF—Ferris dune field; SDF—Seminoe dune field). SL—Separation Lake, the low point in the Great Divide Basin. Arrows indicate flow path of river that previously drained the basin. Cross section A-A′ is used for two-dimensional flexural model (Fig. 2).

the Laramide orogeny (McMillan et al., 2006). These alluvial deposits in areas surrounding the basin reach an elevation of ~2200 m, roughly 250 m above the present spillover point out of the basin. The switch from net aggradation to net incision of Laramide basins in this part of the Rocky Mountains took place after 6.75 Ma, the age of tuffs found at the base of the Moonstone Formation, located just north of the study area in the Granite Mountain block (Anders et al., 2009). Incision of the lowest 100 m of the Great Divide Basin took place over the past 1 m.y., based on the dates and elevations of lava flows found in the Leucite Hills, along the western edge of the basin (Lange et al., 2000). Abandonment of through-going drainage in the basin took place prior to 7 ka, the age of sand dunes shrouding the basin floor. Hence, closure of the Great Divide Basin by a few tens of meters took place between 1 Ma and 7 ka.

Today, the Great Divide Basin's internal drainage consists of ephemeral streams that flow into large playas and small perennial lakes, or disappear beneath active eolian sand dune and sheet deposits. These arid landforms are consistent with modern conditions of low mean precipitation and high mean evaporation rates. Sand dune fields cross into the basin on its western margin, occur on the leeward side of many playas within the basin, and blanket the basin's northeastern margin (Fig. 1). Dune fields trend west to east, parallel to the prevailing westerly wind direction. Winds blow on average 25 km/h in summer and 36 km/h in winter from the west southwest (Martner and Marwitz, 1982). The largest fields include the Killpecker, Seminoe, and Ferris dunes (Fig. 1). The dune fields are as old as latest Pleistocene and have been active throughout the Holocene, with periods of activity coinciding with periglacial conditions (Mayer and Mahan, 2004). Sedimentary and geomorphic evidence from study of the Ferris dune field suggests that wind strength, intensity, and direction have not varied much since the end of the Pleistocene (Gaylord, 1982).

Large playas coincide with the lowest elevations in the basin and broadly define three subbasins separated by ridges of resistant fine-grained sedimentary rocks. The three subbasins include the northwest-southeast–trending Red Desert Basin, an east-west–trending longitudinal valley made up of the Lost Creek Basin, Battle Spring Flat, and Chain Lakes Flat (hereafter identified collectively as the Chain Lakes Flat), and the northwest-southeast–trending Separation Flats (Fig. 1). The Red Desert Basin and Chain Lakes Flat are underlain by the predominantly fluvial and lacustrine deposits of the Tertiary Battle Spring, Wasatch, and Green River formations (Bradley, 1964). Separation Flats is underlain by Upper Cretaceous marine rocks of the Steele Shale, Cody Shale, Mesaverde, and Niobrara Formations (Barlow, 1953; Bayley, 1968).

TOPOGRAPHY

In order to determine where the Great Divide Basin drained prior to closure, we compiled a data set including elevations of divides and other potential overflow points, drainages, and possible burial of such features by eolian sand accumulations from a variety of sources including elevations from U.S. Geological Survey (USGS) digital elevation models (DEMs; 30 m resolution), spot elevations using mapping-grade Trimble differential GPS unit (DGPS) (20 cm resolution after postprocessing), available geologic mapping, and well-log data from the Wyoming Oil and Gas Conservation Commission and Wyoming State Geological Survey.

The average elevation of the Great Divide Basin is 2100 m above mean sea level. Total relief within the basin is significant at ~1100 m difference between the highest point along the crest of the Ferris Mountains (3050 m) and the lowest point in Separation Flats (1947 m). However, on average, the basin is quite flat. Over 80% of the basin area falls within the 1947–2150 m elevation range, and less than 4% of the basin area is above 2300 m above mean sea level. It is important to note that there is very little high topography, and therefore mountain drainage, in the Great Divide Basin catchment (Fig. 1). In contrast, the North Platte drainage, bounding the east and north sides of the basin, drains much of the high topography in this part of the central Rocky Mountains.

Low points in each of the subbasins occur at 2005 m in the Red Desert Basin, 1970 m in the Chain Lakes Flat, and 1947 m in Separation Flats. The lowest points within each subbasin step down in a generally west-to-east pattern. Similarly, the spillover points today between the subbasins step down from west to east from 2038 m between Red Desert Basin and Chain Lakes Flat, to 2005 m between Chain Lakes Flat and Separation Flats, to 1996 m between Separation Flats and the North Platte drainage (Fig. 1).

The lowest gaps along the basin divide (Fig. 1) include Wamsutter Gap (2051 m), Muddy Gap (2066 m), Sinclair Gap (1996 m), and Sand Gap (2097 m). The first three sites have exposed Cretaceous bedrock at the surface, and thus these are minimum spillover elevations. At the Sand Gap site, however, the minimum elevation is located among sand dunes within the Ferris dune field. Sand dunes have blown over Sand Gap and migrated partway down Sand Creek to the north (Fig. 1). Bedrock exposed among the dunes at Sand Gap is at an elevation of 1990 m, which is slightly lower than the elevation of the divide at Sinclair Gap. The largest horizontal distance between bedrock exposures in the Sand Gap area is ~120 m. Therefore, it is possible that sand hides a buried, narrow valley beneath which bedrock basement may be somewhat lower.

Sand Gap seems the most likely outflow from the Great Divide Basin. Not only is bedrock somewhat lower here than at other candidate areas, but Sand Creek, which runs through Sand Gap to join the North Platte River (Fig. 1), has well-developed and extensive high terraces several meters above the current small creek. Bedrock clasts among terrace remnants suggest significant outflow through Sand Creek. These terraces have been partially buried by migrating sand dunes. Thus, a river clearly flowed through the gap prior to the period of Holocene drying. Projection of terrace surfaces suggests that the spillover point at Sand Gap was not much below 1990 m. The maximum relief between the lowest spot in the basin, Separation Lake (at 1947 m), and the bedrock overflow at Sand Gap (1990 m) is 43 m. These sites are located roughly 30 km from each other. It is unclear what generated this closure.

ORIGIN OF BASIN CLOSURE

While there is no known tectonic activity along the northern basin margin, there is evidence of young normal faulting farther to the north, along the northern flank of the Ferris and Seminoe mountains. Love (1970) describes a west-northwest–trending normal fault, the South Granite Mountain fault (SGMF, Fig. 1) that bounds the southern edge of the Granite Mountain block. The structure is near vertical, probably becoming listric with depth (Blackstone, 1991) and places Miocene age deposits (Moonstone Formation) against basement rocks. Displacement along the fault reaches up to 610 m at the far west end of the South Granite Mountain fault (Love, 1970). However, cross sections constrained by well data indicate offset is closer to 200 m around the location of Sand Creek (Love, 1970; Blackstone, 1991). Subparallel faulting along the northern margin of the block (North Granite Mountain fault; Fig. 1) indicates that the Granite Mountains sit in a graben (Love, 1970). Available age constraints indicate that normal faulting began between ca. 11 and 7 Ma, and may be continuing today (Anders et al., 2009). Along the northern flank of the Seminoe Mountains, to the east of Great Divide Basin, truncated spurs provide geomorphic evidence of offset along the fault (Jaworowski, 1985). However, no similar topography is seen in the vicinity of Sand Creek, the proposed outlet of the Great Divide Basin (Fig. 1).

Impact of Extrabasinal Tectonics

It is possible that if there were young, significant normal fault offset along the South Granite Mountain fault, it could have played a role in closing the Great Divide Basin. Normal offset would not close the basin by building a tectonic dam along Sand Creek. In fact, normal fault offset, had it occurred along the drainage, would have led to the formation of a knickpoint, and would have accelerated erosion along the stream, facilitating downcutting. Instead, any significant reduction in tectonic load by thinning of the crust along the margin of the Granite Mountain graben could lead to flexural rebound adjacent to the graben margins. This phenomenon contributes to the formation of "rift shoulders" (Weissel and Karner, 1989; Chéry et al., 1992). Tilting to the south away from the graben would help provide a slope that, under the right conditions, could contribute to closing of the Great Divide Basin.

In order to evaluate this mechanism as a cause of tilting in the eastern Great Divide Basin, we constructed a simple two-dimensional flexural model using cross sections of the Granite Mountains provided by Love (1970). Two-dimensional modeling is appropriate because the load, the Granite Mountain graben, is an elongate feature, and we are modeling a location near the approximate midpoint of the graben margin, so that three-dimensional boundary effects are unlikely to play a significant role. The geologic history of the Granite Mountain block suggests that during, or following, downdrop of basement rocks, sedimentation took place. Assuming the South Granite Mountain fault does not offset the Moho, the result of the net effect of extension and basin filling is to replace basement rock (density ~2850 kg/m^3) with sedimentary rock of density between 2200 and 2500 kg/m^3. Thus, density contrast ranges from 350 to 650 kg/m^3. For simplicity, we assume a rectangular load shape for the graben geometry. Load width is the half-width of the graben, which along our cross section is 24 km. The elastic plate is assumed to be laterally infinite, and thus half the load is compensated for by that part of the plate that extends to the north. For flexural rigidity, we assumed values ranging from 10^{22} to 10^{23} N•m. This range includes the best-fit values for the subsidence geometry of the Cretaceous foreland basin across southern Wyoming (Jordan, 1981; Liu and Nummedal, 2004). Load height is ~200 m based on fault offset of the Split Rock Formation along a cross section near the modern Sand Creek (Love, 1970; Blackstone, 1991). We calculated the resultant relief (tilt) due to rift shoulder development between Sand Gap and Separation Lake (Fig. 2), which lie 30 km apart from each other. Sand Gap is located ~3 km south of the South Granite Mountain fault (Fig. 1). Our estimates of relief were calculated for a variety of likely sediment-fill densities and flexural rigidities. The tilt between Sand Gap and Separation Lake ranges from 2.5 m and 12.4 m, depending on the assumed density and rigidity (Table 1; Fig. 3, white bars). Such values fall far short of the required basement tilt of ~40 m that closes the basin.

Role of Climate Change

The Great Divide Basin today is very dry. The basin has low mean precipitation rates (12–30 cm/yr, avg. 1961–1990; U.S. Department of Commerce, 2005) coupled with high mean evaporation rates (>75 cm/yr of shallow lake evaporation, avg. 1956–1970; Farnsworth et al., 1982). Being on the continental divide,

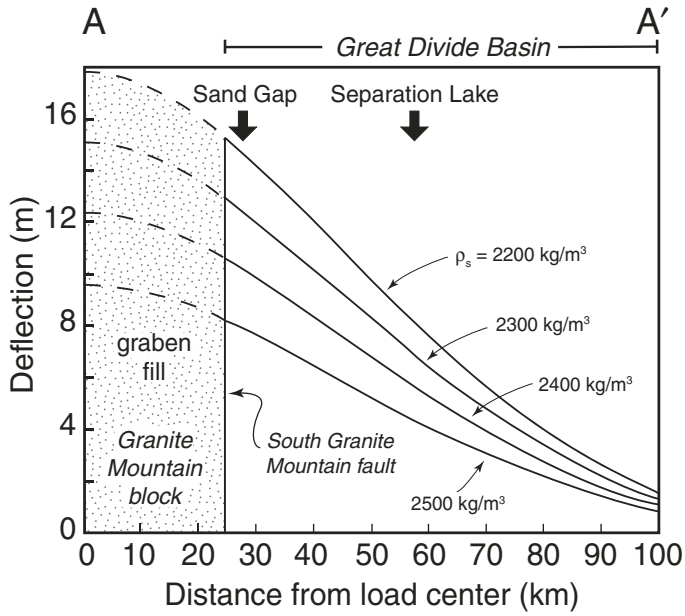

Figure 2. Calculated flexural rebound due to graben development along the Granite Mountain block. Cross section A-A′ (Fig. 1) runs from the Granite Mountain block across the Great Divide Basin. Flexural response is calculated for rigidity of $10^{22.5}$ N•m and assumes that density of sediment filling Granite Mountain graben ranges from 2200 to 2500 kg/m^3, replacing material that is 2850 kg/m^3. Results are calculated for fault offset of 200 m along the South Granite Mountain fault. Solid lines are flexural profiles within Great Divide Basin; dashed lines are profiles within Granite Mountain block. Locations of basin spillover (Sand Gap) and basin low point (Separation Lake) are shown.

TABLE 1. CALCULATED TILT RESULTING FROM RIFT SHOULDER AND REGIONAL EROSION

Flexural rigidity and equivalent effective elastic thickness (EET)	Sedimentary rock density (kg/m^3)	Rift shoulder tilt (relief) from Separation Lake to Sand Gap (M)	Erosional tilt (relief) from Separation Lake to Sand Gap (M)	Total tilt (m)
10^{22} N•m (EET = 11.7 km)	2200	12.4	50.6	63.0
	2300	10.5	56.6	67.1
	2400	8.6	63.7	72.3
	2500	6.7	72.0	78.7
$10^{22.5}$ N•m (EET = 20.0 km)	2200	6.6	27.1	33.7
	2300	5.6	29.7	35.3
	2400	4.6	32.6	37.2
	2500	3.6	35.9	39.5
10^{23} N•m (EET = 25.2 km)	2200	4.7	18.7	23.4
	2300	4.0	20.3	24.3
	2400	3.3	22.2	25.5
	2500	2.5	24.2	29.7

overall elevations are high; however, there is very little relief within the catchment and surrounding range crests. As a result, there is little, if any, orographic impact on prevailing westerly weather fronts to force precipitation within the basin. In contrast, the North Platte River, which flows just east of the basin, originates in the high ranges of northernmost Colorado (Fig. 1). The catchment drains high ranges (>3500 m) where orographic effects promote high precipitation rates (up to >152 cm/yr, avg. 1961–1990; U.S. Department of Commerce, 2005), yielding perennial river flow.

The stark difference in aridity between the adjacent drainages today raises the possibility that change in climate could have impacted the catchments in the past. Specifically, we consider the impact of differential changes in discharge between the Great Divide Basin and adjacent North Platte River drainage during Pleistocene time.

A change in climate alone need not yield any change in differential precipitation between the Great Divide Basin and North Platte River drainages. The nearly ten-fold difference in annual precipitation seen today due primarily to orographic effects could well have existed in Pleistocene time. In the study area, however, Pleistocene glaciation was limited to the headwaters of the North Platte River, with none forming along highlands of the Great Divide Basin (Pierce, 2004). Meltwater was released as glaciers retreated during times of warming climate. This led to periods of high discharge in the Platte river drainage and likely increased erosion. Meanwhile, the absence of glaciers, and thereby significant water storage, in the Great Divide Basin precluded similar magnitudes of stream incision. As a result, rapid downcutting along the Platte River during meltwater times was not matched in the Great Divide Basin—the latter of which was left literally high and dry.

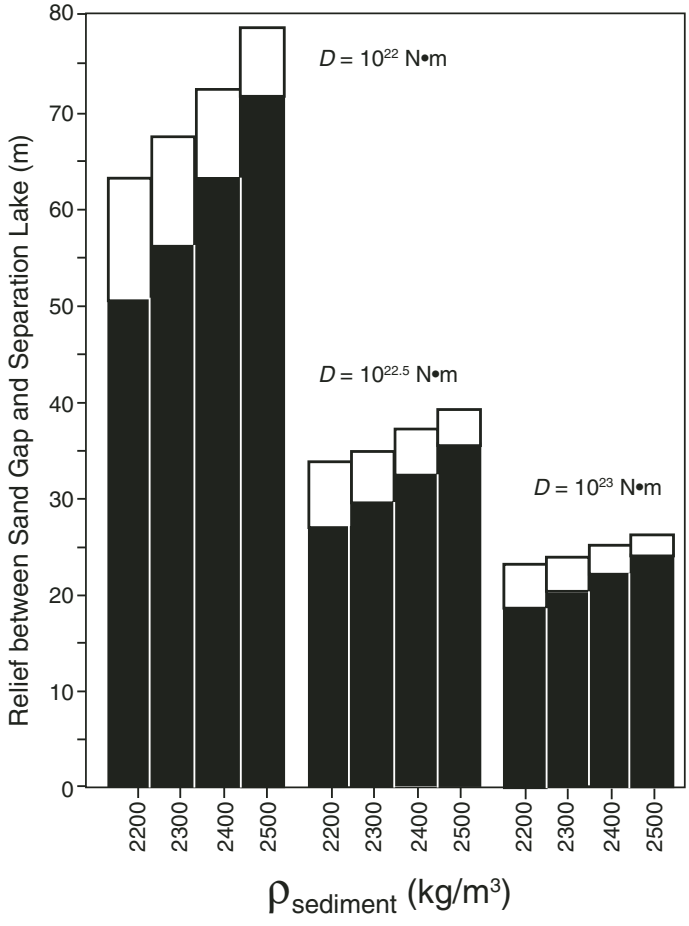

Figure 3. Calculated relative relief between the low point in the basin (Separation Lake) and the inferred spillover point (Sand Gap) due to flexural response related to unloading. Black bars result from removal of deposits along the North Platte River drainage as calculated from the three-dimensional (3-D) flexural model. White bars show tilt due to rift shoulder effects from normal faulting within the Granite Mountain block. Results are for a range of rigidities (10^{22}, $10^{22.5}$, 10^{23} N•m) and assumed density of sedimentary rocks (2200, 2300, 2400, 2500 kg/m^3).

Impact of Extrabasinal Erosion

While the North Platte River continued to erode down to its present position, the Great Divide Basin became abandoned and then closed. The North Platte drainage has eroded a deep, wide valley just northeast of the much higher Great Divide Basin. It therefore seems possible that the strong asymmetry in erosion rates between these drainages may have contributed to closure of the basin due to regional isostatic response (i.e., flexure). Was the flexural uplift due to removal of basin fill in the North Platte drainage enough to lead to the observed differential uplift between Sand Creek Pass and Separation Lake?

In order to evaluate the flexural effect of regional erosion, we applied a three-dimensional elastic flexural model to the northeastern Great Divide Basin, in the vicinity of the Sand Gap spillover point. To facilitate model construction, we assumed that the elevation of the Platte River near where the drainage from the Great Divide Basin once flowed was close to the present elevation of the spillover at Sand Gap, i.e., 1990 m. Thus, we assume that any incision by the North Platte drainage below this elevation took place after the Great Divide Basin was no longer connected to the Platte River. The removal of material below this elevation would then lead to isostatic rebound in the area affected by the flexural effects.

Figure 4 shows the present distribution of the 1990 m contour surrounding the modern Platte River. This contour line is assumed to represent the limits of Platte River erosion since isolation of the Great Divide Basin. We only modeled the region shown in Figure 4, an area of 100 × 120 km. This area includes the northeastern limit of the basin and adjacent parts of the North Platte River drainage from the towns of Rawlins to Casper, Wyoming. This modeled area is closest to the former spillover point at Sand Gap, where flexural impacts would have been greatest. Erosion farther downstream along the North Platte River would have added to the calculated flexural response; however, loads farther away have exponentially less impact on flexure in the area of interest and are considered to have minimal impact on our results.

To facilitate modeling, we broke this region into a series of cylindrical point loads, each 5 km in diameter (Fig. 4), the removal of which leads to flexural rebound. The height of each

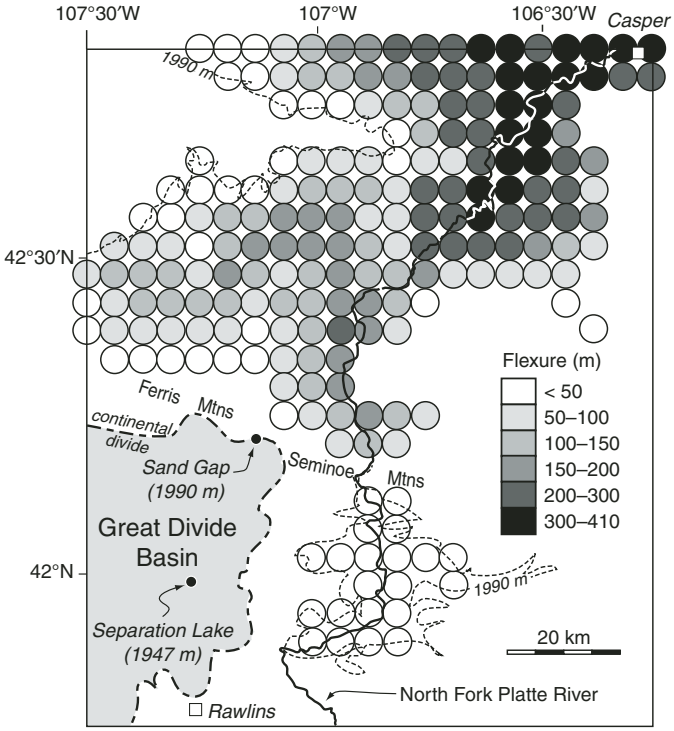

Figure 4. Area modeled in three-dimensional (3-D) flexure analysis. The northeast margin of the Great Divide Basin is shaded. The 1990 m contour (thin dashed line) is model datum. Incision into datum forms the erosional load for model runs. Location and thickness (binned) of eroded cylindrical loads are shown by shaded circles. Position of North Fork of the Platte River, continental divide, and location of the towns of Rawlins and Casper, Wyoming, are shown.

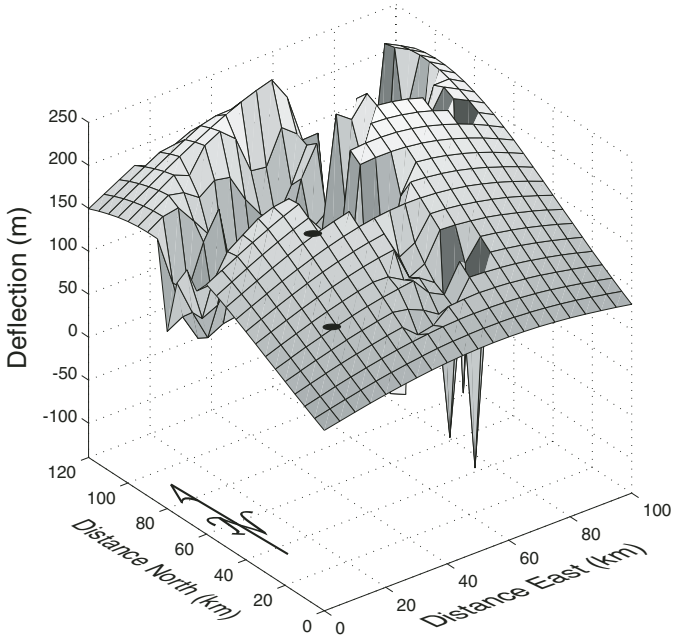

Figure 5. Results of three-dimensional flexural model. Graph shows position of an originally horizontal datum surface following erosion along the North Platte drainage as described in text and resulting flexural rebound ($D = 10^{22.5}$ N•m, $\rho_s = 2500$ kg/m^3). Positions of Sand Gap (to the north) and Separation Lake are shown by black disks.

eroded load was determined from the average elevation of each 5-km-square grid point over which these cylinders were centered. We calculated the difference between average elevation of each cell and the 1990 m datum representing the preerosion surface. The erosion of each grid point is available in the GSA Data Repository,[1] but the general heights of each load, binned, are shown in Figure 4.

Our flexural model assumes the elastic plate was infinite in all directions. Model runs used a range of densities of eroded sedimentary rock (2200–2500 kg/m^3) and flexural rigidities (10^{22}–10^{23} N•m, equivalent to effective elastic thickness of 12–25 km; Table 1). An example of a calculated flexural response to removal of the eroded material using a flexural rigidity of $10^{22.5}$ N•m is shown in Figure 5. Both the shape and magnitude of doming associated with regional erosion are shown. In the area of analysis, rebound generates between 19 and 50 m of relief, depending on assumed flexural rigidity value and the density of eroded material (Table 1). The model assumes that topography of the area prior to erosion was that of a flat surface at 1990 m. Therefore, we ignore any erosion that might have taken place in the preexisting mountains surrounding the region, which would only serve to increase the possible amount of rebound and tilt. Thus, we consider the model response to be a minimum estimate at that flexural rigidity.

DISCUSSION

In order to explain the basin closure with ~40 m of relief between the basin low point and the spillover at Sand Gap by flexural response, either the assumption of low flexural rigidity is required for the erosional model alone, or for the combined isostatic effects of regional erosion as well as tilting due to rifting to the north (Fig. 3; Table 1). We find that if we use the best-fit flexural rigidity determined by analysis of Cretaceous foreland basin deflection in southern Wyoming ($10^{22.5}$ N•m; Liu and Nummedal, 2004), we get excellent agreement with the observed relief of basin closure in the Great Divide Basin (34–40 m depending upon sedimentary rock density assumed; Fig. 3). An increase in flexural rigidity to 10^{23} N•m yields insufficient rebound to explain the observed relief (Table 1).

The flexural model described here has little impact on the paleoelevations of the other candidate overflow points. The position of Sand Gap, in the NE corner of the basin, allows it to

[1]GSA Data Repository item 2010158, Table of load magnitudes, is available at http://www.geosociety.org/pubs/ft2010.htm or by request to editing@geosociety.org.

be maximally impacted by both the area of greatest erosion along the North Platte River to the northeast and the normal faulting to the north. We have not observed any other erosional or tectonic patterns in the vicinity of the other potential overflow points around the basin that would yield comparable results from flexural modeling.

It is possible that some additional relief may have been generated by local wind deflation in the area of Separation Lake. We have observed occasional ventifact clasts in this part of the basin. Wind erosion on the order of 10 m would make it possible for the higher rigidity to provide a reasonable fit. Regardless, we find it interesting that rigidity of $10^{22.5}$ N•m best explains both the Cretaceous subsidence history of southern Wyoming as well as our Pleistocene to Holocene reconstruction. This suggests there has been little net change in regional rigidity over the past ~70 m.y. across southern Wyoming, despite the Laramide crustal thickening that occurred during this time.

Model of Basin Evolution

Our results suggest that climate, leading to low erosion rates in the Great Divide Basin in contrast to high erosion rates nearby, coupled with an isostatic flexural response can explain basin closure and most of the relief between the basin low point and spillover point. A key factor to this interpretation is that the Great Divide Basin, once tributary to the North Platte River, is arid and has very little potential to integrate much precipitation despite its large size. None of the ranges surrounding the basin has high enough relief to force much orographic precipitation today. In addition, none of the ranges has large enough catchment area to provide significant discharge to the basin.

During Pleistocene time, glaciers that formed in the headwaters of the North Platte River (Fig. 6), but not in the Great Divide Basin, provided a means for high discharge during meltwater events during periods of glacial retreat (e.g., Pelletier, 2009). Accelerated erosion along the North Platte River, but not the Great Divide Basin outflow, led to isolation of the latter from the Platte drainage. Erosion in excess of 200 m by the North Platte River led to isostatic rebound that flexed the northeast corner of the Great Divide Basin, creating significant relief in the area of the basin outlet (i.e., tens of meters), which forced basin closure. Rigidities of the order $10^{22.5}$ N•m generated a broad doming that affected the entire eastern part of the basin as well as nearby areas (Fig. 6). In addition, normal faulting along the Granite Mountain block to the north of the Great Divide Basin (SGMF in Fig. 6) that took place sometime in the past <11 m.y. encouraged minor back tilting due to flexural rift shoulder effects. This added to closed basin relief, albeit to a minor extent.

Finally, windblown dunes formed as a result of continued aridification of the central Rockies and adjacent Great Plains over Holocene time (Marrs et al., 1987). Dune fields are common along the Wyoming Wind Corridor, which runs east across the southern half of Wyoming including the Great Divide Basin. A discontinuous line of sand dunes can be traced across the basin into the area of the basin outlet at Sand Gap (Fig. 1). Sand dunes bank around the northeast basin margin and overtop the divide into the adjacent Platte River drainage. The dunes add as much as an extra ~100 m of relief to the basin closure in the area of Sand Gap.

CONCLUSIONS

Two- and three-dimensional flexural analysis suggests that closure of the Great Divide Basin was likely due to enhanced erosion in the adjacent North Platte River drainage. Enhancement of

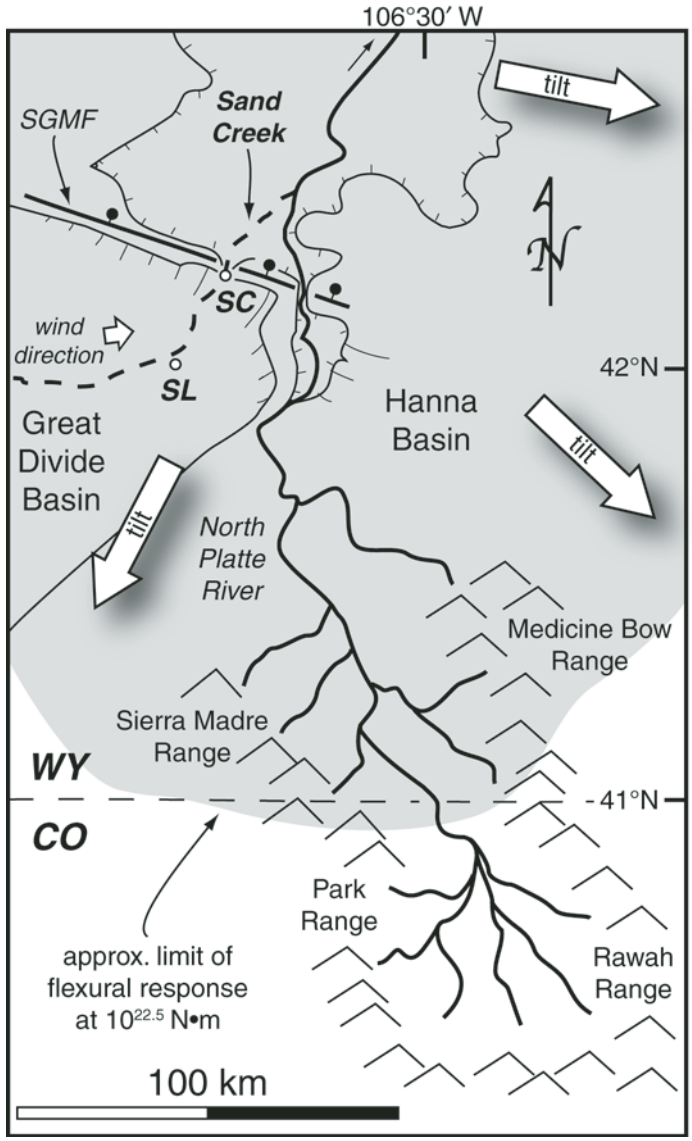

Figure 6. Key elements for interpretation of climatic cause of closure of the Great Divide Basin. Shaded region shows approximate area that underwent flexural response and unloading due to erosion by the North Platte River (assuming flexural rigidity of $10^{22.5}$ N•m) as well as thinning of the Granite Mountain block. Heavy dashed line follows approximate trace of previous drainage out of Great Divide Basin. SC—Sand Creek Gap, SL—Separation Lake.

this closure was due to minor extrabasinal tectonic impact and the encroachment of sand dunes due to increased aridification in Holocene time. In our model, differential erosion is caused by increased meltwater discharge during periods of deglaciation. Headwaters of the North Platte River were glaciated; the Great Divide Basin was not.

Because of the competition between the effects of rift shoulder and erosional tilt, the results are not very sensitive to the sediment density assumed. The greater is the sediment density, the more erosional rebound plays a role, and the less rift shoulder uplift contributes. The amount of calculated tilt is sensitive to the flexure rigidity of the lithosphere, producing a good fit with observed basin relief if a rigidity of $10^{22.5}$ N•m is used. This value is the best fit found by Liu and Nummedal (2004) in their study of Cretaceous foreland basin development across the same part of Wyoming. Hence, this suggests that net regional flexural rigidity has not changed over the intervening ~70 m.y.

Isostatic impacts caused by differential erosion may play roles in drainage reorganizations and basin closure, and locally enhance structural features in a variety of locales (e.g., Simpson, 2004). Deep incision of the Grand Canyon by the Colorado River has led to in excess of 300 m of flexural rebound (Pelletier, 2010). With broad wavelength deformation on the scale of 100 km, flexural rebound may have led to drainage reorganization and drainage reversal along the canyon rim. Similarly, Qinghai Lake, the largest lake in China, sits near the northeast margin of the Tibetan Plateau. The lake sits in a shallow closed basin that may owe its origins to basin closure due to nearby erosion by the Yellow River.

Our results indicate that the presence of a closed basin does not require, nor should be taken as proof of, tectonic activity. Flexural response to moderate differential erosion, as seen in this analysis, can generate tens of meters of tilt over wavelengths of many tens of kilometers. Such modest topography is sufficient to close basins in most settings. An even greater degree of closure would have occurred if more incision had taken place. Although perhaps atypical, it seems that under special circumstances, climate alone can lead to closed basin formation.

ACKNOWLEDGMENTS

Field assistance was graciously provided by Peter Beland, Max Garnier, Steve Holbrook, and Cliff Riebe. We thank Xiangyang Xie for allowing us to use his three-dimensional flexure program, and PASSCAL (IRIS) and Bryan Shuman for use of geophysical equipment used to determine depth to bedrock. We benefited from discussions with Bryan Shuman and reviews by Peter Molnar and Christian Koeberl. Funding was made available through the Petroleum Research Fund of the American Chemical Society.

REFERENCES CITED

Anders, M.H., Saltzman, J., and Hemming, S.R., 2009, Neogene tephra correlations in eastern Idaho and Wyoming: Implications for Yellowstone hotspot-related volcanism and tectonic activity: Geological Society of America Bulletin, v. 121, p. 837–856, doi: 10.1130/B26300.1.

Barlow, J.A., 1953, The Geology of the Rawlins Uplift, Carbon County, Wyoming [Ph.D. thesis]: Laramie, University of Wyoming, 179 p.

Bayley, R.W., 1968, Geologic Map of the Bradley Peak Quadrangle Carbon County, Wyoming: Washington, D.C., U.S. Geological Survey, 1 sheet.

Blackstone, D.L., Jr., 1991, Tectonic Relationships of the Southeastern Wind River Range, Southwestern Sweetwater Uplift, and Rawlins Uplift, Wyoming: Laramie, Geological Survey of Wyoming, 24 p.

Bradley, W.H., 1964, Geology of Green River Formation and associated Eocene rocks in southwestern Wyoming and adjacent parts of Colorado and Utah: U.S. Geological Survey Professional Paper 496-A, p. 1–86.

Carroll, A.R., and Bohacs, K.M., 1999, Stratigraphic classification of ancient lakes: Balancing tectonic and climatic controls: Geology, v. 27, p. 99–102, doi: 10.1130/0091-7613(1999)027<0099:SCOALB>2.3.CO;2.

Chéry, J., Lucazeau, F., Daignières, M., and Vilotte, J.P., 1992, Large uplift of rift flanks: A genetic link with lithospheric rigidity?: Earth and Planetary Science Letters, v. 112, p. 195–211, doi: 10.1016/0012-821X(92)90016-O.

Farnsworth, R.K., Thompson, E.S., and Peck, E.L., 1982, Evaporation atlas for the contiguous 48 United States, *in* NOAA Technical Report 33: Washington, D.C., Office of Hydrology, National Weather Service, National Oceanic and Atmospheric Administration, U.S. Department of Commerce, p. 26BI.

Flanagan, K.M., and Montagne, J., 1993, Neogene stratigraphy and tectonics of Wyoming, *in* Snoke, A.W., Steidtmann, J.R., and Roberts, S.M., eds., Geology of Wyoming, Volume 5: Laramie, Geological Survey of Wyoming, p. 572–607.

Garcia-Castellanos, D., 2007, The role of climate during high plateau formation; insights from numerical experiments: Earth and Planetary Science Letters, v. 257, p. 372–390, doi: 10.1016/j.epsl.2007.02.039.

Gaylord, D.R., 1982, Geologic history of the Ferris dune field, south-central Wyoming, *in* Marrs, R.W., and Kolm, K.E., eds., Interpretation of the Windflow Characteristics from Eolian Landforms: Geological Society of America Special Paper 192, p. 65–82.

Hansen, W.R., 1986, Neogene tectonics and geomorphology of the eastern Uinta Mountains in Utah, Colorado and Wyoming: U.S. Geological Survey Professional Paper 1356, p. 1–78.

Humphrey, N.F., and Konrad, S.K., 2000, River incision or diversion in response to bedrock uplift: Geology, v. 28, p. 43–46, doi: 10.1130/0091-7613(2000)28<43:RIODIR>2.0.CO;2.

Jaworowski, C.C., 1985, Geomorphic Mapping and Trend Analysis of Quaternary Deposits with Implications for Late Quaternary Faulting, Central Wyoming Laramie [M.S. thesis]: University of Wyoming, 109 p.

Jordan, T.E., 1981, Thrust loads and foreland basin evolution, Cretaceous, western United States: American Association of Petroleum Geologists Bulletin, v. 65, p. 2506–2520.

Keller, G.R., and Baldridge, W.S., 1999, Lithospheric structure and evolution of the Rocky Mountains: Part II: Rocky Mountain Geology, v. 34, p. 121–130, doi: 10.2113/34.1.121.

Lange, R.A., Carmichael, I.S.E., and Hall, C.M., 2000, $^{40}Ar/^{39}Ar$ chronology of the Leucite Hills, Wyoming: Eruption rates, erosion rates, and an evolving temperature structure of the underlying mantle: Earth and Planetary Science Letters, v. 174, p. 329–340, doi: 10.1016/S0012-821X(99)00267-8.

Lillegraven, J.A., and Ostresh, L.M., Jr., 1988, Evolution of Wyoming's early Cenozoic topography and drainage patterns: National Geographic Research, v. 4, p. 303–327.

Lillegraven, J.A., Snoke, A.W., and McKenna, M.C., 2002, Tectonic and paleogeographic implications of late Laramide geologic history in the northeastern corner of Wyoming's Hanna Basin: Rocky Mountain Geology, v. 39, p. 7–64, doi: 10.2113/39.1.7.

Liu, S., and Nummedal, D., 2004, Late Cretaceous subsidence in Wyoming: Quantifying the dynamic component: Geology, v. 32, p. 397–400, doi: 10.1130/G20318.1.

Love, J.D., 1970, Cenozoic Geology of the Granite Mountains Area, Central Wyoming: Washington, D.C., U.S. Geological Survey, 154 p.

Marrs, R.W., Kolm, K.E., and Gaylord, D.R., 1987, Dunes of the Wyoming Wind Corridor, southern Wyoming, *in* Stanley, S.B., Rocky Mountain section of the Geological Society of America: Boulder, Colorado, Geological Society of America, Centennial Field Guide, Rocky Mountain Section, p. 209–212.

Martner, B.E., and Marwitz, J.D., 1982, Wind characteristics in southern Wyoming: Journal of Applied Meteorology, v. 21, p. 1815–1827, doi: 10.1175/1520-0450(1982)021<1815:WCISW>2.0.CO;2.

Mayer, J.H., and Mahan, S.A., 2004, Late Quaternary stratigraphy and geochronology of the western Killpecker dunes, Wyoming: Quaternary Research, v. 61, p. 72–84, doi: 10.1016/j.yqres.2003.10.003.

McMillan, M.E., Heller, P.L., and Wing, S.L., 2006, History and causes of post-Laramide relief in the Rocky Mountain orogenic plateau: Geological Society of America Bulletin, v. 118, p. 393–405, doi: 10.1130/B25712.1.

Mears, B., Jr., 1998, Neogene normal faulting superposed on a Laramide uplift: Medicine Bow Mountains, Sierra Madre, and intervening Saratoga, Wyoming and Colorado: Contributions to Geology (Copenhagen), v. 32, p. 181–185.

Mederos, S., Tikoff, B., and Bankey, V., 2005, Geometry, timing and continuity of the Rock Springs Uplift, Wyoming, and Douglas Creek Arch, Colorado: Implications for uplift mechanisms in the Rocky Mountain foreland, U.S.A.: Rocky Mountain Geology, v. 40, p. 167–191, doi: 10.2113/40.2.167.

Pelletier, J.D., 2009, The impact of snowmelt on the late Cenozoic landscape of the southern Rocky Mountains, USA: GSA Today, v. 19, no. 7, p. 4–11, doi: 10.1130/GSATG44A.1.

Pelletier, J.D., 2010, Numerical modeling of the late Cenozoic geomorphic evolution of Grand Canyon, Arizona: Geological Society of America Bulletin, v. 122, p. 595–608.

Pierce, K.L., 2004, Pleistocene glaciations of the Rocky Mountains, *in* Gillespie, A.R., Porter, S.C., and Atwater, B.F., eds., The Quaternary Period in the United States: Developments in Quaternary Science: Amsterdam, Elsevier, p. 63–76.

Simpson, G., 2004, Role of river incision in enhancing deformation: Geology, v. 32, p. 341–344, doi: 10.1130/G20190.2.

Snoke, A.W., 1993, Geologic history of Wyoming within the tectonic framework of the North American Cordillera, *in* Snoke, A.W., Steidtmann, J.R., and Roberts, S.M., eds., Geology of Wyoming, Volume 5: Laramie, Geological Survey of Wyoming, p. 2–56.

Surdam, R.C., and Stanley, K.O., 1980, Effects of changes in drainage-basin boundaries on sedimentation in Eocene lakes Gosiute and Uinta of Wyoming, Utah, and Colorado: Geology, v. 8, p. 135–139, doi: 10.1130/0091-7613(1980)8<135:EOCIDB>2.0.CO;2.

U.S. Department of Interior, 2009, National Atlas: Precipitation of the Individual States and of the Conterminous States: http://www.nationalatlas.gov/index.html; http://www.nationalatlas.gov/printable/precipitation.html#list (accessed 2 April 2009).

Weissel, J.K., and Karner, G.D., 1989, Flexural uplift of rift flanks due to mechanical unloading of the lithosphere during extension: Journal of Geophysical Research, v. 94, p. 13,919–13,950, doi: 10.1029/JB094iB10p13919.

Manuscript Received 20 June 2009
Revised Manuscript Received 2 February 2010
Manuscript Accepted 4 February 2010

Printed in the USA